The EMBO Journal (2006) 25, 2498–2509 | © 2006 European Molecular Biology Organization | All Rights Reserved 0261-4189/06
www.embojournal.org

THE EMBO JOURNAL

Structure of the unusual seryl-tRNA synthetase reveals a distinct zinc-dependent mode of substrate recognition

Silvija Bilokapic[1], Timm Maier[2], Dragana Ahel[1,3], Ita Gruic-Sovulj[1], Dieter Söll[3], Ivana Weygand-Durasevic[1,*] and Nenad Ban[2,*]

[1]Department of Chemistry, University of Zagreb, Zagreb, Croatia, [2]Institute of Molecular Biology and Biophyscis, Swiss Federal Institute of Technology, ETH Zürich, ETH Hoenggerberg, Zürich, Switzerland and [3]Department of Molecular Biophysics and Biochemistry, Yale University, New Haven, CT, USA

Methanogenic archaea possess unusual seryl-tRNA synthetase (SerRS), evolutionarily distinct from the SerRSs found in other archaea, eucaryotes and bacteria. The two types of SerRSs show only minimal sequence similarity, primarily within class II conserved motifs 1, 2 and 3. Here, we report a 2.5 Å resolution crystal structure of the atypical methanogenic *Methanosarcina barkeri* SerRS and its complexes with ATP, serine and the non-hydrolysable seryl-adenylate analogue 5′-*O*-(*N*-serylsulfamoyl)adenosine. The structures reveal two idiosyncratic features of methanogenic SerRSs: a novel N-terminal tRNA-binding domain and an active site zinc ion. The tetra-coordinated Zn^{2+} ion is bound to three conserved protein ligands (Cys306, Glu355 and Cys461) and binds the amino group of the serine substrate. The absolute requirement of the metal ion for enzymatic activity was confirmed by mutational analysis of the direct zinc ion ligands. This zinc-dependent serine recognition mechanism differs fundamentally from the one employed by the bacterial-type SerRSs. Consequently, SerRS represents the only known aminoacyl-tRNA synthetase system that evolved two distinct mechanisms for the recognition of the same amino-acid substrate.

The EMBO Journal (2006) **25,** 2498–2509. doi:10.1038/sj.emboj.7601129; Published online 4 May 2006
Subject Categories: RNA; structural biology
Keywords: protein synthesis; RNA; tRNA synthetases; X-ray crystallography

Introduction

In all organisms seryl-tRNA synthetases (SerRS) have the essential role of aminoacylating cognate $tRNAs^{Ser}$ with serine (Ibba and Söll, 2000; Weygand-Durasevic and Cusack, 2005). These enzymes also serylate selenocysteine-specific tRNAs ($tRNA^{Sec}$) and thus participate in the incorporation of selenocysteine into proteins (Baron and Bock, 1995). SerRS is a homodimeric enzyme belonging to the class II aminoacyl-tRNA synthetases (aaRSs), characterized by a catalytic domain with an antiparallel β-sheet architecture comprising three conserved motifs: 1, 2 and 3 (Cusack *et al*, 1990; Eriani *et al*, 1990; Fujinaga *et al*, 1993; Chimnaronk *et al*, 2005). On the basis of extensive sequence analysis, SerRS was subsequently subclassified as a class IIa synthetase together with AlaRS, ThrRS, ProRS, HisRS and homodimeric GlyRS (Cusack *et al*, 1991; Cusack, 1993; Ribas de Pouplana and Schimmel, 2001), although it lacks the C-terminal anticodon-binding domain characteristic of all other class IIa synthetases.

SerRS is one of the very few synthetases that do not specifically recognize the tRNA anticodon. Instead, the major identity element of $tRNA^{Ser}$ and $tRNA^{Sec}$, shared among procaryotic, eucaryotic and archaeal systems, is a long variable arm. Accordingly, SerRS enzymes have acquired a unique N-terminal domain for variable arm recognition (Borel *et al*, 1994; Vincent *et al*, 1995). In this regard, the only known exception is the metazoan mitochondrial $tRNAs^{Ser}$/SerRS system, whose tRNA structures markedly deviate from the canonical cloverleaf secondary structure with highly truncated and/or intrinsically missing arms (Helm *et al*, 2000). Consequently, biochemical (Shimada *et al*, 2001) and recent structural studies (Chimnaronk *et al*, 2005) have revealed that the tRNA binding specificity of mammalian mitochondrial SerRS differs from all other known SerRS systems.

A series of crystal structures of binary and tertiary complexes involving *Thermus thermophilus* SerRS (Tt-SerRS), followed by a high-resolution crystal structure of an *Escherichia coli* SerRS (Ec-SerRS) arm-deletion mutant in complex with a seryl-adenylate analogue, explained the specificity and mechanism of serine activation by bacterial SerRSs (Belrhali *et al*, 1994, 1995; Weygand-Durasevic and Cusack, 2005). Serine specificity is ensured firstly by the small size of the side-chain pocket (which permits exclusion of threonine) and secondly by the interaction of the serine side-chain hydroxyl group with that of Thr380 in motif 3 of Tt-SerRS or Ser391 of Ec-SerRS. Furthermore, a conserved motif 2 glutamate residue (Glu279 Tt-SerRS and Glu239 in Ec-SerRS, respectively) makes simultaneous hydrogen bonds to the α-amino and hydroxyl group of the serine substrate. This feature efficiently excludes alanine and thus bacterial SerRSs do not require an editing activity. The availability of SerRS sequences from a number of organisms from all three domains permitted a detailed analysis of the phylogeny of this enzyme (Lenhard *et al*, 1999; Wolf *et al*, 1999; Woese *et al*, 2000). SerRS is phylogenetically of particular interest

*Corresponding authors. N Ban, Institute of Molecular Biology and Biophyscis, Swiss Federal Institute of Technology, ETH Zurich, ETH Hoenggerberg, HPK Bld., Zurich 8093, Switzerland.
Tel.: +41 1 633 27 85; Fax: +41 1 633 12 46;
E-mail: ban@mol.biol.ethz.ch or
I Weygand-Durasevic, Department of Chemistry, Faculty of Science, University of Zagreb, Horvatovac 102a, Zagreb 10 000, Croatia.
Tel.: +385 1 460 6230; Fax: +385 1 460 6401; E-mail: weygand@irb.hr

Received: 24 January 2006; accepted: 11 April 2006; published online: 4 May 2006

 ©2006 European Molecular Biology Organization

primarily because there are two distinct serine-charging enzymes: a standard or canonical type of SerRS was found in the majority of organisms (procaryotes, eucaryotes and archaea), while a highly diverged SerRS is confined to the methanogenic archaea (*Methanococcales*), with the exception of *Methanosarcina mazei* and *Methanosarcina acetivorans* (Tumbula *et al*, 1999; Korencic *et al*, 2002). Interestingly, the two distinct types of SerRSs coexist in *Methanosarcina barkeri* (Korencic *et al*, 2004b).

In accordance with the noted disparity between bacterial and methanogenic types of SerRSs (Kim *et al*, 1998), our previous results indicated that the two types of *M. barkeri* enzymes do not possess a uniform mode of $tRNA^{Ser}$ recognition (Korencic *et al*, 2004b). Furthermore, unlike bacterial-type *M. barkeri* SerRS, the methanogenic enzyme is sensitive to serinamide inhibition, suggesting mechanistic differences in serine recognition (Ahel *et al*, 2005).

In order to elucidate the structural basis for the observed divergence between the two types of SerRSs, we have determined the structure of the methanogenic *M. barkeri* SerRS (aMb-SerRS) at 2.5 Å resolution and compared it with structures of bacterial-type counterparts from *E. coli* (Cusack *et al*, 1990), *T. thermophilus* (Fujinaga *et al*, 1993) and mammalian (*Bos taurus*) mitochondria (Chimnaronk *et al*, 2005). We have also determined structures of the unusual methanogenic SerRS in complex with substrates and substrate analogues representing different steps in the serine activation reaction. Finally, the role of selected amino acids in the serylation reaction was confirmed by structure-based mutagenesis. The observed mechanism of serine recognition, which differs from the one employed by the bacterial-type SerRSs, is reminiscent of the zinc ion-based amino-acid discrimination used by threonyl-tRNA synthetases (Dock-Bregeon *et al*, 2000; Sankaranarayanan *et al*, 2000) and as such provides a link to a common class II aaRS ancestor with evolving amino-acid specificities. We propose that the distinction between the two types of SerRSs, displayed at the level of amino-acid sequence, three-dimensional structure and substrate recognition mechanism, reflects their divergent evolutionary pathway within a group of otherwise highly conserved enzymes.

Results

The X-ray crystal structure of the methanogenic *M. barkeri* SerRS was determined at 2.5 Å resolution, as well as structures of the enzyme with either ATP, serine or 5′-*O*-(*N*-(L-seryl)sulfamoyl)adenosine (Ser-AMS) at 2.2, 2.7 and 2.4 Å resolution, respectively. The crystals contained two molecules per asymmetric unit. The structure is complete, except for a few loops (12–20, 52–56, 84–95) within the N-terminal domain of one subunit, which displays higher flexibility in general. Data collection and refinement statistics are summarized in Supplementary Table S1.

The overall structure

The two molecules in the asymmetric unit form a homodimer, consistent with the dimeric nature of all other known SerRSs (Borel *et al*, 1994; Vincent *et al*, 1995; Gruic-Sovulj *et al*, 1997; Bilokapic *et al*, 2004). The overall structure and topology of aMb-SerRS are illustrated in Figure 1. Each

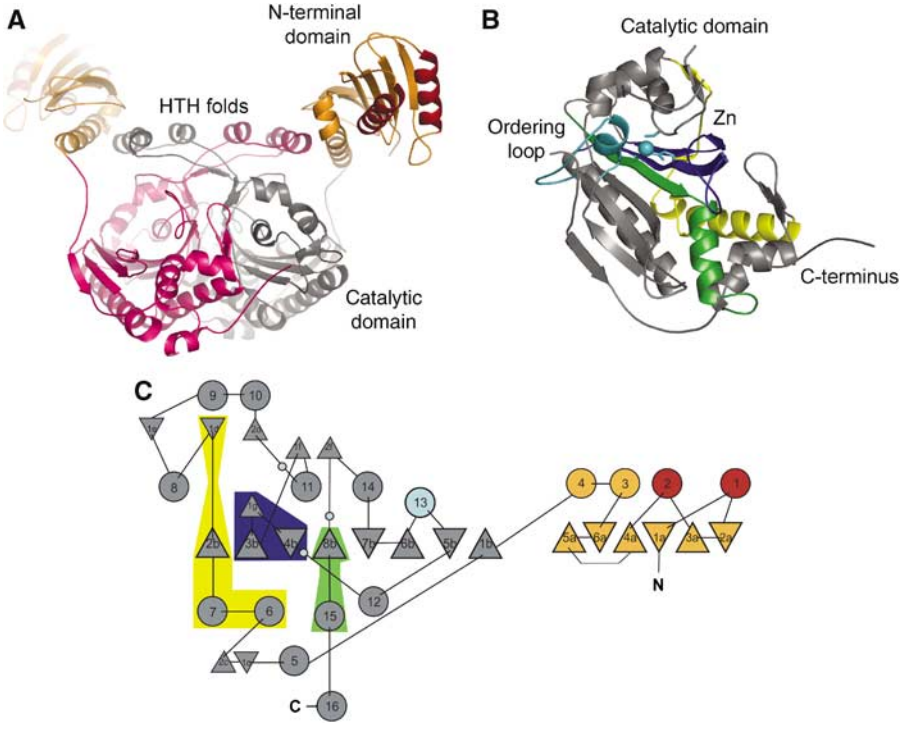

Figure 1 Overall structure of SerRS from *M. barkeri*. (**A**) Ribbon diagram of the overall crystal structure of aMb-SerRS showing the catalytic core of the two subunits in pink and gray, respectively. The novel RNA-binding domain is in orange with helices proposed to be involved in RNA binding highlighted in red. The noncrystallographic symmetry two-fold axis is in the plane of the paper. (**B**) Catalytic domain of aMb-SerRS with three class II signature motifs 1, 2 and 3 colored in yellow, blue and green, respectively. Zinc atom and its amino-acid ligands are shown in cyan, as well as the 'serine ordering loop' (residues 394–410). (**C**) Topology of the enzyme. Domains and motifs are colored as in (A) and (B). Secondary structure elements are labelled.

©2006 European Molecular Biology Organization

monomer consists of two distinct domains, a catalytic core and an N-terminal extension, as also observed for bacterial-type SerRSs (Cusack *et al*, 1991; Cusack, 1993).

The structure of aMb-SerRS reveals several features unique to methanogenic SerRS. A striking difference between the two SerRS types is apparent in the N-terminal domain, which is significantly larger in methanogenic-type enzymes (Figure 2). In aMb-SerRS, this domain is composed of a six-stranded antiparallel β-sheet (a1–a6) capped by a bundle of three helices (H1, H2, H4) with up-down topology and an additional short helix (H3) that runs almost perpendicular to helix H4 (Figure 1A and C). In contrast, the N-terminal domain of the bacterial-type SerRS consists only of two long antiparallel helices forming a coiled coil. Despite the observed structural difference, N-terminal domains of all SerRS counterparts are presumably involved in tRNA binding and are similarly positioned relative to the catalytic domain.

The catalytic core domain of *M. barkeri* SerRS, which comprises an eight-stranded β-sheet flanked by α-helices, shares a common organization with all other known SerRSs structures (Cusack *et al*, 1990; Fujinaga *et al*, 1993; Chimnaronk *et al*, 2005). However, the active site of the catalytic domain differs significantly from other SerRSs and includes a metal ion, as revealed by the inspection of anomalous difference Fourier maps. Analysis of X-ray absorption spectra identified this ion as zinc. Considering that zinc ions were not introduced during purification or crystallization, they must be tightly bound by aMb-SerRS. The refined structure reveals that a single zinc ion is coordinated with the side chains of Cys306, Glu355 and Cys461 (Figure 1B). A water molecule completes the tetrahedral coordination of the zinc. This feature indicates that this zinc site is catalytic rather than structural, where the metal coordination sphere is commonly saturated with protein side chains. As explained below, the zinc-bound water dissociates from the zinc ion to allow for coordination of a substrate, which is essential for catalysis. This water is additionally coordinated by main chain oxygen of Ala304 that is not in the zinc primary coordination sphere.

The biological significance of the zinc ion is emphasized by the strict conservation of each of the protein ligands throughout all methanogenic-type SerRSs. Two other aaRSs contain zinc in the active site: these are ThrRS (class II) and CysRS (class I). Sequence alignment reveals that zinc binding residues in ThrRS (Cys334, His385 and His511 in *E. coli* ThrRS) and in the methanogenic-type SerRSs have an equivalent location in the primary sequence (Figure 2).

Besides the differences in the design and chemistry of the active site, further dissimilarities between typical and atypical SerRSs are observed in various structural elements. Specifically, the motif 2 loop is several amino acids shorter in the methanogenic-type SerRSs than in their counterparts from other organisms (Figures 1 and 2). Furthermore, the methanogenic-type SerRSs are characterized by the presence of several insertions that render their alignment to the bacterial-type SerRS sequences difficult (Figure 2). All SerRSs of methanogenic type possess a unique stretch of ~30 amino acids positioned between motifs 1 and 2. The structure reveals that these residues adopt a helix–turn–helix (HTH) fold, which is in intimate contact with the core and the N-terminal domain of the second subunit in the homodimer. This interaction simultaneously locks the two cores together through intertwining of the helices and presents a charged surface of one of the helices for the formation of a series of salt bridges with helix H4 of the N-terminal tRNA-binding domain. Secondary structure predictions indicate the existence of the same motif in all methanogenic-type SerRS, suggesting an important role of this motif for interdomain interactions. The second insertion in the catalytic domain of methanogenic-type SerRS is found between motifs 2 and 3 (positions 394–410 in aMb-SerRS; 'serine ordering loop') (Figures 1B, C and 2). This peptide stretch corresponds to the 'threonine loop' in ThrRS, which shifts upon threonine binding in ThrRS (Torres-Larios *et al*, 2003) and fulfils a similar role in serine binding here (see below) (Figure 2).

ATP-binding site

The structure of the *M. barkeri* SerRS complexed with ATP (Figure 3A and B) reveals that this substrate is bound in the active site in a manner characteristic for class II synthetases. In the binary complex, the adenine ring of ATP is stacked between the aromatic ring of Phe351 and the guanidinium group of Arg468, both invariant residues in motifs 2 and 3, respectively. Additionally, ATP is further stabilized in its position by interactions with the main chain oxygen of Val348 and the carboxylate of the Glu338 side chain. Its ribose is in the 3′-endo conformation and the 3′OH is engaged in a hydrogen bond with the invariant Glu432. The ATP 2′-hydroxyl interacts with the carbonyl oxygen of Phe433. With ATP in the bent conformation, the β and γ phosphates are folded back towards the adenine ring into a U-shaped structure, which is consistent with an in-line S_N2 mechanism of amino-acid activation in class II aaRS. This conformation is achieved through interactions of the phosphates with protein side chains, mediated by bridging magnesium ions, which were assigned based on proximity to phosphate groups and by analogy to other class II synthetases. The α and β phosphates coordinate a magnesium ion, which is bound to the side chains of Asp416, Glu432 and Asn435. The β and γ phosphates are bridged to Glu338 and N7 of the ATP adenosine ring at the opposite side by another magnesium ion. Arg468 and Arg347 provide additional stabilization of the γ phosphate, and Arg336 interacts with the α phosphate. The residues maintaining contacts with ATP are conserved

Figure 2 Structure-based sequence alignment of aMb-SerRS with selected SerRS sequences from all kingdoms of life and with catalytic domains of closely related ThrRSs. The sequence alignment was firstly generated using the program ClustalX (Thompson *et al*, 1997) and then manually adjusted based on structural considerations. The sequences are derived from archaea (Mm, *Methanococcus maripaludis*; Mt, *Methanothermobacter thermoautotrophicus*; Mk, *Methanopyrus kandleri*; Mb, *Methanosarcina barkeri*; Mbu, *Methanococcoides burtonii*), bacteria (Tt, *Thermus thermophilus*; Ec, *Escherichia coli*) and eucarya (Sc, *Saccharomyces cerevisiae*; Hs, *Homo sapiens*). One mitochondrial sequence (Bt, *Bos taurus*) was also included. Amino acids that are completely conserved are in red, whereas those with 80 and 60% conservation are in orange and yellow, respectively. Secondary structural elements are indicated above the alignment with red cylinders for helices and blue arrows for β-sheets. Residues important for zinc ion coordination in aMb-SerRS are marked with asterisks. A green arrow indicates mitochondrial signal sequence. Conserved class II motifs 1, 2 and 3, as well as methanogenic type specific HTH motif, are labeled.

 ©2006 European Molecular Biology Organization


A1
H1
A2
A3
H2
A4
A5
A6
H3
H4
MOTIF 1
B1
H5
C1
C2
H6
H7
B2
D1
H8
HELIX-LOOP-HELIX
MOTIF 2
E1
H9
H10
D2
H11
F1
B3
G1
B4
H12
B5
H13
B6
B7
H14
MOTIF 3
F2
B8
H15
H16
Tt-SerRS
Ec-SerRS
Sc-SerRS
Hs-SerRS
Bt-mSerRS
Mm-SerRS
Mt-SerRS
Mk-SerRS
aMb-SerRS
Mbu-SerRS
Tt-ThrRS
Ec-ThrRS
Sc-ThrRS
Hs-ThrRS

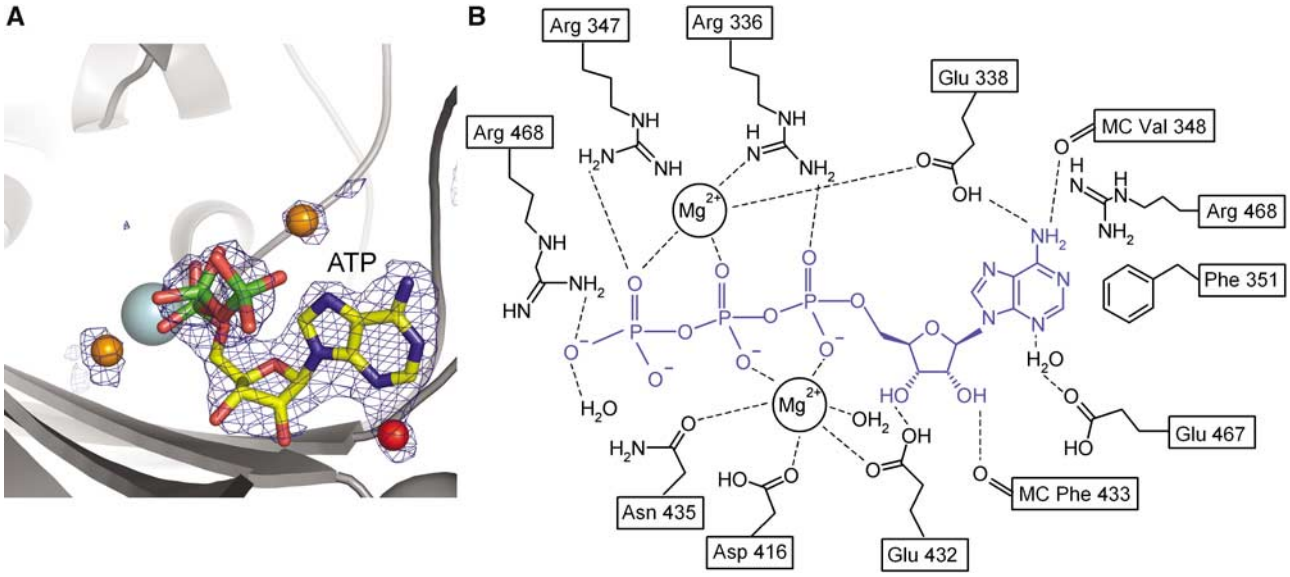

Figure 3 ATP binding by SerRS. (**A**) Simulated annealing omit F_o-F_c electron density map (resolution 2.0 Å, contour level 2.7σ) together with the refined model: ATP, magnesium ions and surrounding atoms within a sphere of 3 Å were omitted from the model during map calculation. The protein is shown as a ribbon in gray, zinc ion is in cyan, bound magnesium ions and water molecules are shown as orange and red spheres, respectively. The bound ligand is shown in a ball-and-stick representation. (**B**) Schematic representation of the interactions between the enzyme, ATP and magnesium.

or conservatively substituted in all methanogenic and bacterial-type SerRSs (Figure 2).

Serine-binding site

Upon serine binding, the coordination of the active site zinc ion by amino-acid side chains remains intact, whereas the water ligand is replaced by the serine amino group (Figure 4A). Hence, the zinc coordination sphere remains tetrahedral with bound serine. The amino group of serine is additionally stabilized by hydrogen bonding with the main chain oxygen of Ala304. The structure reveals that Glu355, which is conserved between the methanogenic and bacterial-type SerRSs (Figure 2), has a dual role in the methanogenic enzyme: in addition to being a zinc ligand, it interacts with the hydroxyl group of the serine substrate, as in the bacterial-type SerRS. The side-chain hydroxyl of serine is further constrained by the conserved Arg353.

Owing to the striking divergence between typical and methanogenic SerRS and the unexpected similarity between methanogenic SerRS and ThrRSs, we have performed alanine-scanning mutagenesis of Cys306, Glu355 or Cys461 in aMb-SerRS to confirm the importance of residues identified as direct zinc ion ligands. Our results showed that substitution of these amino acids yielded enzymatically inactive protein, confirming the importance of the zinc ion in serine recognition. Given that Cys306 and Cys461 are not conserved in the bacterial-type enzymes, their role in the selection of amino-acid substrate is indicative in terms of the evolutionary origin of SerRSs in relation to other class II enzymes.

The binding of serine changes the conformation of the 'serine ordering loop', comprising residues 394–410, which is completely disordered in its absence. The conformational change brings the loop in the proximity of the zinc ion and enables a direct contact between Gln400 and the carbonyl oxygen of the serine substrate (Figure 4). Although the interactions with Gln400 seem important, the residue is not conserved in all methanogenic-type SerRSs; possibly, Arg in sequences of other methanogenic-type SerRSs performs an analogous function. Furthermore, in the binary complex, Trp396 packs above the amino group of the serine substrate and hence binding of noncognate amino acids would sterically prevent the ordering loop from adopting an active conformation. We accordingly suggest that Trp396 acts as a gatekeeper and plays an important role in determining the size of the amino-acid binding pocket. This residue is not fully conserved among the methanogenic-type SerRSs, but its replacement by Phe in some methanogenic SerRSs would permit similar interactions.

Interestingly, bacterial-type SerRSs possess a shorter loop at the position equivalent to the 'serine ordering loop'. However, a substrate-induced structural transition occurs only in methanogenic-type SerRSs, where it results in helix formation in the N-terminal part of the ordering loop and presumably contributes to amino acid selectivity. In conclusion, amino-acid specificity in aMb-SerRS depends on the availability of the β-hydroxyl group in the amino-acid substrate and on the size of the binding pocket. Analogously, the binding of threonine to ThrRS leads to the movement of the polypeptide chains 417–466 (Torres-Larios *et al*, 2003), which is structurally equivalent to the 'serine ordering loop' in aMbSerRS. This results in the formation of a hydrogen bond between Tyr462 and the threonine α-amino group. Moreover, Tyr462 switches from the recognition of the amino acid to that of the 2′-hydroxyl of the terminal adenosine when tRNA is bound.

Seryl–adenylate complex

A nonhydrolysable analogue of Ser-AMS, soaked into the active site, was visualized in difference Fourier electron density maps and in a simulated-annealing omit map (Figure 4B). The adenosine ring and serine moiety of AMS display the same pattern of interactions with the protein

 ©2006 European Molecular Biology Organization

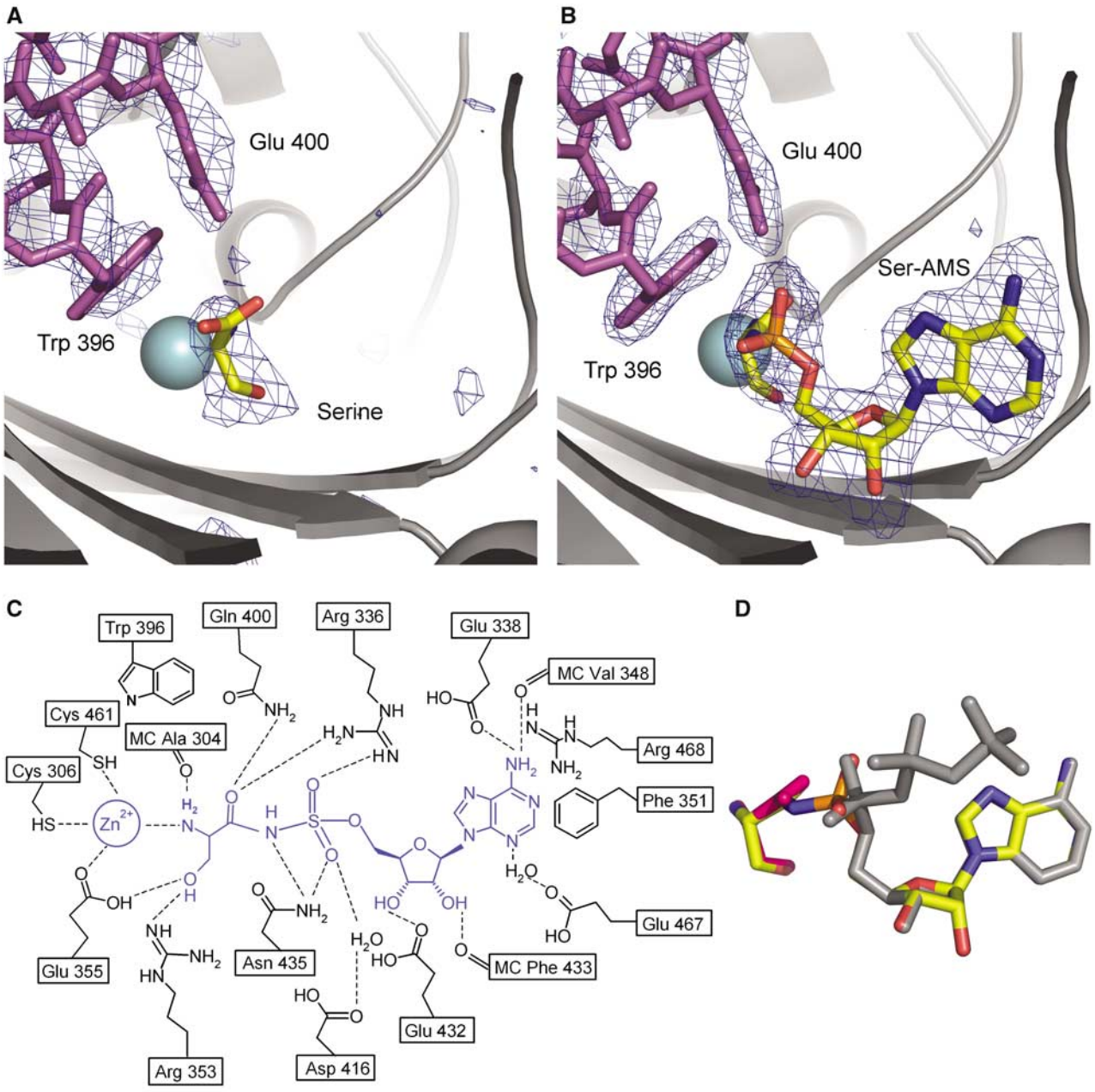

Figure 4 Active site of aMb-SerRS occupied with (**A**) serine (resolution 2.7 Å, contour level 2.1σ) and (**B**) seryl-adenylate analogue Ser-AMS (resolution 2.5 Å, contour level 2.2σ). Simulated annealed omit F_o-F_c map calculation as for Figure 3A, orientation and colors are chosen as in Figure 3. Magenta main and side chains undergo serine-induced conformational changes. (**C**) Schematic representation of the interactions between the enzyme and Ser-AMP. (**D**) The superposition of Ser-AMS, ATP and serine bound to the active site of aMb-SerRS. ATP is colored in gray, serine in pink and Ser-AMS in an atom-type coloring scheme.

as the corresponding parts of the serine and ATP substrates in the binary complexes (Figure 4C). The serine carboxylate is well positioned for an in-line attack on the α-phosphate of ATP.

Arg336, invariant in class II aaRS, interacts with one of the sulfate oxygens and the carbonyl oxygen of Ser-AMS, whereas the other sulfate oxygen interacts with Asn435. The carbonyl oxygen of the serine part is additionally coordinated with Gln400, which again interacts with His250 (Figure 4C). Interestingly, His250 occupies a position equivalent to His204 in the Tt-SerRS structure, which is engaged in an indirect contact to the carboxyl oxygen of the serine substrate; this contact is mediated by a water molecule positioned equivalently to the Gln400 carbamide in the aMb-SerRS structure.

In contrast to three class I synthetases, the glutamyl-, glutaminyl- and arginyl-tRNA synthetases, SerRS catalyzes the first step of the aminoacylation reaction in the absence of the cognate tRNA(s) and therefore the bound serine and ATP are in an equivalent position as observed for their corresponding parts in the seryl–adenylate complex. The geometry of the substrates in the active site and the surrounding amino acids are in agreement with the previously proposed in-line

©2006 European Molecular Biology Organization

displacement reaction mechanism (Belrhali *et al*, 1995; Arnez *et al*, 1999) (Supplementary Figure S2).

Amino-acid selectivity and misactivation

Considering the unusual nature of the active site of the methanogenic SerRS, we have investigated the possibility of amino-acid misactivation by threonine and cysteine using an ATP-PP_i exchange assay. Interestingly, serine can bind into the active site of ThrRS through interactions with the zinc ion and ThrRS shows detectable misactivation of serine (Sankaranarayanan *et al*, 2000; Dock-Bregeon *et al*, 2004). Therefore, we were interested in examining the level of discrimination against threonine achieved by the aMb-SerRS. Our results show slight but notable misactivation of threonine with a discrimination factor $\{1/[(k_{cat}/K_{m,Thr})/(k_{cat}/K_{m,Ser})]\}$ of 3450 (Table I). Interestingly, both SerRS and ThrRS showed the same 10^3-fold decrease in K_m for the noncognate substrate, threonine and serine, respectively. On the contrary, significant decrease in k_{cat} for noncognate activation was observed for SerRS, but not ThrRS (Table I and Sankaranarayanan *et al* (2000)). Threonine chemically and structurally resembles serine and its β-hydroxyl and α-amino groups could be positioned in the active site as the corresponding parts of serine. However, superposition of Thr-AMS onto Ser-AMS in the complex with aMb-SerRS shows that binding of threonine in the same orientation as serine would induce clashes between the threonine methyl and the sulfhydryl group of Cys461. Therefore, in order to avoid steric clashes, threonine probably adopts a conformation that is less efficient in promoting an in-line attack of the reactive oxygen of the carboxylate group. In addition to steric incompatibility, binding of noncognate threonine would be energetically disfavored as the accommodation of its methyl group requires displacement of a structurally conserved water molecule, coordinated by Asn435 and Ser437, from the ligand-binding site. Our experiments revealed that misactivated threonine is (apparently) not edited by the aMb-SerRS, either by tRNA-dependent or tRNA-independent route, as no stimulation of ATP hydrolysis (Baldwin and Berg, 1966; Tsui and Fersht, 1981) was observed when threonine substituted serine in the reaction mixture, independent of the presence of tRNA. On the other hand, cysteine is only barely misactivated by the aMb-SerRS, as shown by pyrophosphate exchange experiments. The observed catalytic constant (k_{obs}) at 500 mM amino-acid concentration was 15 times lower for cysteine than for threonine (Table I). Inefficiency of cysteine activation by the aMb-SerRS can be attributed to steric hindrance. If cysteine were to replace serine in the active site of aMb-SerRS, the cysteine sulfhydryl group would clash with Glu355, which consequently prevents cysteine binding.

The role of the HTH motif for stability and tRNA binding

M. barkeri SerRS contains a unique HTH fold inserted into the catalytic core between motifs 1 and 2 (Figures 1 and 2). The structure reveals that the HTH motif from one monomer is crossing the two-fold axis of the dimer and is positioned above the catalytic domain of the other monomer (Figure 5A). The HTH motifs from the two subunits in the dimeric aMb-SerRS are nearly parallel with respect to each other and form a four-helix cap covering the two catalytic cores. Furthermore, the two outermost helices of the cap are engaged in a series of salt bridges and hydrogen bond interactions with the last helix (H4) of the N-terminal domain (Figure 5B). Many DNA-binding proteins include an HTH motif with the two helices perpendicular to each other (Wintjens and Rooman, 1996). However, the two helices of the HTH motif in the aMb-SerRS structure have no structural similarity with this motif owing to their parallel arrangement. The position of the HTH motif and its interactions with helix 4 strongly suggests that the function of this motif is to assist proper positioning of the tRNA-binding domain.

Furthermore, in addition to the class II conserved motif 1, the HTH fold significantly increases the dimer interface in the aMb-SerRS; helix 9 interacts with its dimer symmetry-related counterpart and helix 10 interacts with helix 4 in the N-terminal domain of the companion monomer. This increases the total surface area in the dimer interface from 2010 $Å^2$, contributed by motif 1, to 3760 $Å^2$ per monomer. It is likely that these additional interactions and the larger contact area results in an increased stability of the aMb-SerRS dimer compared to its bacterial counterpart. Such stabilization could be of biological significance, considering that many methanogenic archaea are thermophilic organisms and/or live in special environments.

Interactions with tRNA

In order to gain an initial understanding of the interaction between SerRS and its cognate tRNA, we have used the bacterial SerRS-$tRNA^{Ser}$ complex structure (Biou *et al*, 1994) to model tRNA binding onto aMb-SerRS (Figure 6A). Catalytic cores of dimeric aMb-SerRS were superimposed onto the corresponding part of the *T. thermophilus* SerRS-$tRNA^{Ser}$ complex. As part of the $tRNA^{Ser}$ in the *T. thermophilus* co-crystal structure is disordered, for the ease of visualization we further superimposed a nearly complete structural model of $tRNA^{Tyr}$ (Yaremchuk *et al*, 2002), comprising a long variable arm, onto the $tRNA^{Ser}$ (Figure 6B). The two tRNAs have a very similar fold, but the position of the variable arms differs significantly. Despite obvious limitations of such a docking model, which precludes detailed discussions, a number of general conclusions about tRNA

Table I Kinetic parameters obtained in ATP-PP_i exchange assay

	K_m (M)	k_{cat} (s^{-1})	k_{cat}/K_m ($s^{-1}\,M^{-1}$)	$(k_{cat}/K_m)_{relative}$
Serine	$(104 \pm 27) \times 10^{-6}$	1.7 ± 0.1	$(16.4 \pm 3) \times 10^3$	1
Threonine	$(65 \pm 19) \times 10^{-3}$	0.3 ± 0.03	4.7 ± 1.5	2.9×10^{-4}
Cysteine	ND	0.01[a]	ND	ND

ND, not determined.
Calculated discrimination factor $[1/(k_{cat}/K_m)_{relative}]$ is 3450.
[a]This is an observed catalytic constant (k_{obs}) at 500 mM cysteine.

 ©2006 European Molecular Biology Organization

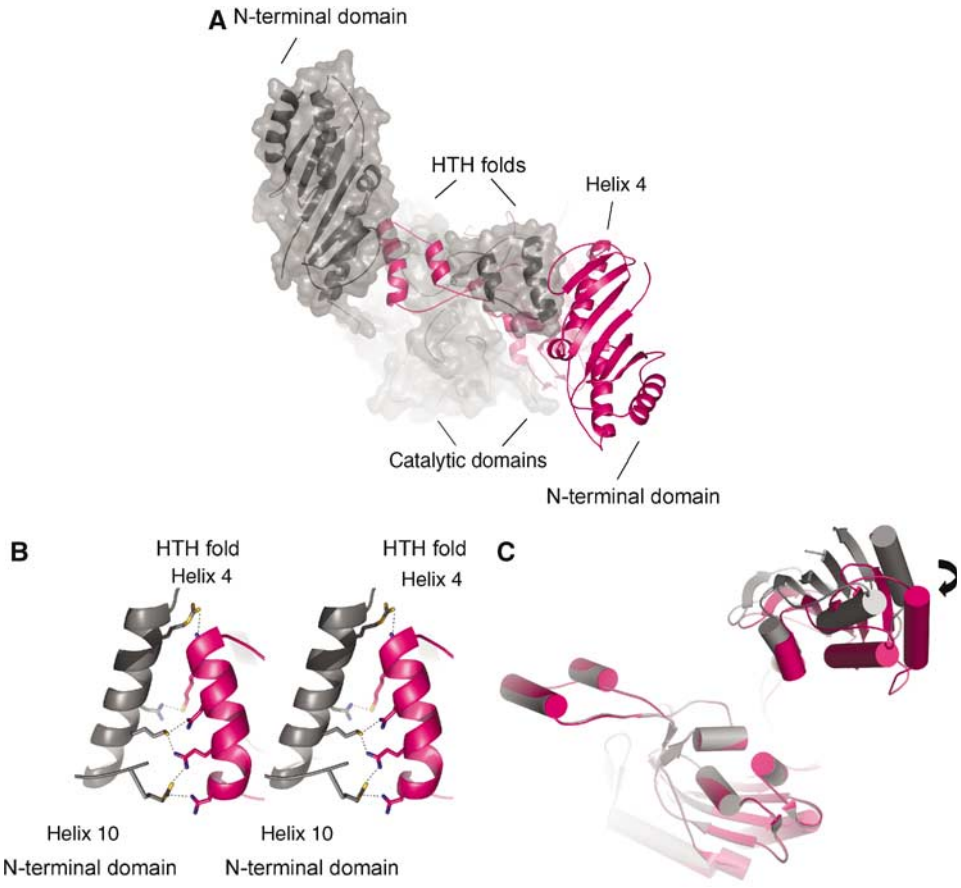

Figure 5 Intersubunit interactions and the role of the HTH motif. (**A**) A view along the two-fold axis with a dimer in ribbon representation. Additionally, transparent surface representation is shown for one monomer. The view highlights the cross-subunit contacts mediated by the HTH fold. The monomers are shown in pink and gray. (**B**) Stereoview of interacting residues between HTH fold from one monomer and the N-terminal domain from the symmetry related subunit. The same color code is used as in (A). (**C**) The superposition of the two subunits, in gray and magenta, by means of the catalytic domain. The figure demonstrates the hinge movement of the tRNA-binding domain and its different orientation with respect to the catalytic core. The view looking down the rotation axis shows that orientation of this domain in two monomers differs by a rotation of $\sim 20^{\circ}$.

recognition by aMb-SerRS can be drawn. The mode of tRNA binding across two subunits of dimeric enzyme, as observed in the bacterial SerRS-tRNA^{Ser} complex, appears conserved in aMb-SerRS. In the model, the long variable arm of the tRNA is positioned to interact with the highly conserved helices H1 and H2 of the N-terminal domain of aMb-SerRS, in accordance with our previous biochemical experiments, which identified the long variable arm of archaeal tRNA^{Ser} as a major tRNA recognition determinant (Bilokapic *et al*, 2004; Korencic *et al*, 2004b). Electrostatic potential calculations of the SerRS dimer show an extended area of positive surface potential on the inner bow of the N-terminal domain in the general area of helices H1 and H2 (Figure 6C), which is probably involved in the recognition of the negatively charged tRNA backbone.

The tRNA-binding domain occupies a different position in each monomer. Once the catalytic cores of both monomers are superimposed, a hinge-type movement by about 20° (around an axis nearly parallel with H4) is required to superimpose the tRNA-binding domains (Figure 5C). This flexibility of the tRNA-binding domain in the tRNA-free state suggests the relevance of an opening–closing motion of this domain relative to the catalytic core for tRNA binding. The current model suggests that despite structural differences between the two types of SerRS, the tRNA^{Ser} binds to the enzyme in an analogous manner.

Discussion

Dynamic aspects of substrate recognition

The aMb-SerRS structures described here suggest that the small substrates enter the active site before tRNA binding and rearrange the conformation of the peptide inserted between canonical motifs 2 and 3 (the 'serine ordering loop'; Figures 2 and 4). Prior to small substrate binding, this loop is disordered and could interfere with tRNA binding. In that way, serine-induced conformational change may be a signal for tRNA^{Ser} binding and for triggering the second step of the aminoacylation reaction (Supplementary Figure S1). Conformational change induced by binding of small substrates that leads to productive tRNA binding has been previously observed for some aaRS, as ThrRS and CysRS (Torres-Larios *et al*, 2003; Hauenstein *et al*, 2004).

The selection of amino-acid substrate relies both on the interactions with protein side chains and the stably bound zinc ion (Figures 1 and 4). Upon serine binding, the 'ordering loop' is stabilized in a productive conformation: Trp396 packs against the serine amino group, and a hydrogen bond is

©2006 European Molecular Biology Organization

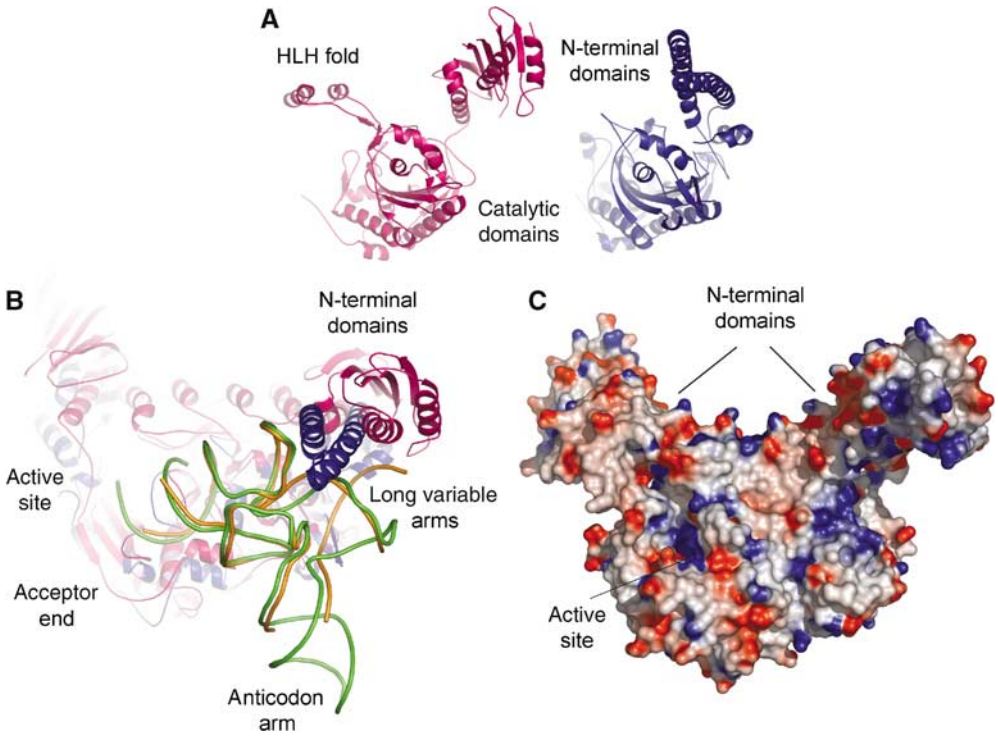

Figure 6 Docking model of tRNA onto Mb-SerRS. (**A**) Comparison of the overall fold and domain arrangement in the two SerRS representatives: single subunit of atypical (aMb-SerRS in pink) and bacterial (Ec-SerRS in blue) SerRS. Structurally homologous catalytic domains of both SerRSs are in the same orientation. (**B**) Proposed model of tRNA binding. Two SerRS representatives are shown as dimers and in the same color code as in (A). $tRNA^{Ser}$ is colored orange and $tRNA^{Tyr}$ green. The position of the $tRNA^{Tyr}$ is obtained after superimposition on the core of $tRNA^{Ser}$. The figure shows that a hinge movement, as indicated by an arrow, of the *M. barkeri* N-terminal domain would be required to reach the long variable arm of the $tRNA^{Ser}$. (**C**) Solvent accessible surface representation of the aMb-SerRS dimer colored by electrostatic potential (red for negative and blue for positive) suggests regions involved in the interactions with the negatively charged phosphate backbone of the tRNA molecule.

formed between Gln400 and the carboxyl oxygen of the serine (Figure 4). These motions are required to position the carboxylate oxygen for the nucleophilic attack onto the α-phosphate of ATP. The presence of an ordering loop structure is a common mechanism that ensures the specificity of several class II synthetases (Yaremchuk *et al*, 2001). While serine and histidine binding is sufficient for the conformational ordering of a short loop in the active site of SerRS and HisRS, formation of prolyl-adenylate is required for ordering in ProRS. In Tt-GlyRS, the topologically equivalent loop also moves upon cognate amino-acid binding, but the loop itself, as it is the case in ThrRS, does not interact with the substrate directly (Arnez *et al*, 1999). Such conformational transition induced by amino-acid binding is in contrast with some other aaRSs whose pocket for the cognate amino-acid side chain is largely preformed (Yaremchuk *et al*, 2001 and references therein).

Discrimination against threonine

The active site zinc ion participates in the amino-acid selection in ThrRS and methanogenic-type SerRS. This similarity in the mechanism is matched by the similarity in primary sequence positioning of the invariant zinc ligands (Cys306, Glu355 and Cys461 in aMb-SerRS, and Cys334, His385 and His511 in Ec-ThrRS; Sankaranarayanan *et al*, 2000), indicated with asterisks in Figure 2. However, a comparison of aMbSerRS-Ser-AMS complex with the structures of the Tt-SerRS and Ec-ThrRS in complex with their respective amino-acyl adenylate analogs reveals that the hydroxyl group of the serine moiety is positioned in a way characteristic for SerRS. In the crystal structures of three SerRSs (*T. thermophilus*, *B. taurus* and *M. barkeri*) the amino-acid hydroxyl groups are constrained by conserved glutamic acid residues in the active site (Glu279 in Tt-SerRS, Glu355 in aMb-SerRS and Glu335 in Bt-SerRS). The active site zinc ion in ThrRS interacts with both the side-chain hydroxyl groups and the main chain amino groups of the amino-acid substrate, resulting in a different position of the hydroxyl group and, consequently, a different orientation of the amino-acid substrate than in the aMb-SerRS structures (Supplementary Figure S2). These differences in the mechanism of zinc-mediated amino-acid discrimination by methanogenic SerRS and ThrRS, the only other class II synthetase that binds zinc in the active site, are suggested to result in a different level of noncognate amino-acid discrimination by the two synthetases.

While ThrRS significantly misactivates serine (discrimination factor 1100; Sankaranarayanan *et al*, 2000), the level of threonine misactivation by aMb-SerRS (discrimination factor 3450) approximates the proposed tolerable limit. Binding of threonine in the active site of methanogenic SerRS would position its methyl group towards Cys461 and a hydrophilic environment built around Asn435 and Ser437, the latter coordinating a structural water molecule. Although bacterial-type SerRS does not employ a zinc-mediated mechanism of serine recognition, the structural basis of discrimination against threonine is similarly based on the formation of

 ©2006 European Molecular Biology Organization

a hydrophilic environment around the conserved residues Ser348 and Asn378, which is repelling the threonine methyl group, as proposed by Belrhali *et al* (1994, 1995). In contrast, the threonine methyl group in ThrRS is stabilized by hydrophobic contacts with the invariant residues Thr482 and Ala513.

Compared to the methanogenic-type SerRS, initial selection of amino-acid substrate in ThrRS is less discriminative (Sankaranarayanan *et al*, 2000). However, the accuracy of protein synthesis is in this case maintained through editing activity, either in *cis* (Dock-Bregeon *et al*, 2000; Beebe *et al*, 2004) or in *trans* (Korencic *et al*, 2004a). Regarding methanogenic-type SerRSs, the biological significance of the threonine misactivation observed *in vitro* also depends on intracellular concentrations of the respective amino acids. Therefore, since aMb-SerRS does not correct misactivated threonine *in vitro*, it remains uncertain whether *trans* editing of mischarged $tRNA^{Ser}$ is necessary *in vivo*.

Homology modelling of tRNA onto M. barkeri SerRS

Methanogenic SerRS is divided into a catalytic core domain and an N-terminal tRNA-binding domain, which are connected by a 9-residue linker helix. Our model for the enzyme in complex with tRNA shows that flexibility of the N-terminal domain is required for optimal binding of the long variable arm of $tRNA^{Ser}$ (Figures 5C and 6A, B). However, detailed understanding of the interaction between the synthetase and tRNA will require further crystallographic studies of the complex. Interestingly, tRNA-binding domains in the two SerRS types are nonhomologous and evolutionarily unrelated. Still, the requirement for a closing motion of the N-terminal domain upon tRNA binding (Figure 6A–C) has also been observed in the *T. thermophilus* SerRS-tRNA co-crystal structure (Biou *et al*, 1994; Cusack *et al*, 1996). Our biochemical data (Bilokapic *et al*, 2004; Korencic *et al*, 2004b) revealed that bacterial $tRNA^{Ser}$ can be recognized by the methanogenic SerRSs, indicating that both N-terminal modules have the same function and similar specificity. This indicates that at least some aspects of tRNA recognition are conserved between the two SerRS types. This observation may be compared to the fact that bacterial and eucaryotic GlyRS enzymes possess homologous catalytic cores, but their tRNA-binding domains are very different in sequence and tertiary structure (Tang and Huang, 2005). Nevertheless, both can recognize the same $tRNA^{Gly}$.

Evolutionary origin of methanogenic SerRSs

Among class IIa enzymes, SerRS, ProRS and ThrRS are structurally and phylogenetically related and form the Ser-Thr-Pro supercluster (Woese *et al*, 2000) of aaRSs. This grouping is substantiated by the structural similarity of their amino-acid substrates: serine and threonine are obviously structurally related, and share a capacity to form an internal hydrogen-bonded five-membered ring structure that mimics the structure of proline. Moreover, serine, threonine and proline have related codons with an NCN consensus, which accentuates the evolutionary relatedness within this distinct subgroup of aaRSs.

Whereas bacterial SerRSs and all ProRSs possess a TxE motif implicated in substrate recognition (Thr225 and Glu227 in the *T. thermophilus* SerRS structure), ThrRSs are characterized by a highly conserved KPMNCP loop that entails an absolutely conserved cysteine (Cys334 in the *E. coli* ThrRS). Interestingly, Cys306 in the *M. barkeri* SerRS belongs to a conserved AQCXPF motif, structurally equivalent to the KPMNCP motif in ThrRSs (Sankaranarayanan *et al*, 2000).

On the other hand, motif 3 of methanogenic SerRSs diverges more substantially from the ThrRS sequence; instead, it resembles motif 3 of bacterial-type ProRSs, possessing a conserved CxGFG sequence (Cys461 in the *M. barkeri* SerRS and Cys443 in *E. coli* ProRS). Accordingly, similarities between methanogenic SerRS, ThrRS and bacterial-type ProRS sequences may be suggestive of an ancient origin of methanogenic SerRS, which possibly retained particular characteristics of the active site architecture that pertained to the common ancestor of the Ser-Thr-Pro supercluster. An alternative possibility is that methanogenic SerRS is a specialized type of SerRS designed to meet particular requirements of methanogenic archaea. In this respect, it is noteworthy that phylogenetic occurrence of methanogenic SerRS coincides with the absence of canonical CysRS (with the exception of *M. maripaludis*), known to utilize zinc-amino-acid recognition. Cys-$tRNA^{Cys}$ formation in the majority of methanogenic archaea was recently shown to proceed via an indirect pathway, which involves *O*-phosphoseryl-$tRNA^{Cys}$ (Sep-$tRNA^{Cys}$) formation by *O*-phospho-SerRS, and subsequent conversion of Sep-$tRNA^{Cys}$ to Cys-$tRNA^{Cys}$ (Sauerwald *et al*, 2005). The ancestral origin of this pathway has been invoked and seems to support the idea that some features that characterized ancient aminoacyl-tRNA synthesis were retained in the methanogenic milieu.

In conclusion, zinc-mediated serine recognition employed by methanogenic SerRS shows that the SerRS system is the only known aaRS system that developed two fundamentally different types of amino-acid recognition. Considering that methanogenic SerRS and ThrRS use a zinc ion for amino-acid discrimination and that both enzymes misactivate threonine and serine, respectively, we may hypothesize that the mechanism of zinc ion-dependent amino-acid recognition predates segregation of SerRS and ThrRS into enzymes with distinct specificities. These assumptions concur with the concept of an ancient origin proposed for methanogenic SerRS.

Materials and methods

Purification and crystallization

The recombinant protein was purified by expression in *E. coli*, followed by Ni_2^+-chelating, cation-exchange and gel-filtration chromatography. Crystals were obtained with 50 mM MES/KOH, pH 5.9, 6.5% MPD, at 19°C. Prior to freezing, the crystals were gradually transferred into mother liquor solution containing 23% (v/v) MPD. Sequence assignment in the flexible N-terminal part of the chain was confirmed by collecting anomalous data from a selenomethionine-derivatized protein containing an Ile77Met mutation. Details of the purification are provided in Supplementary data.

Structure determination and refinement

Crystallographic data were processed using HKL suite (Otwinowski and Minor, 1997) software. The structure was solved using selenomethionine-derivatized protein. Data from a three-wavelength MAD experiment were used to locate 24 selenium sites in SHELXD (Sheldrick and Schneider, 1997) and to calculate initial phases. The resulting phases were refined with density modification using DM (Collaborative Computational Project, 1994; Cowtan, 1994) including solvent flattening. The RESOLVE (Terwilliger, 2002) program located several secondary structural elements in the initial electron density map and superposition of the Tt-SerRS catalytic

©2006 European Molecular Biology Organization

domain onto these partially traced secondary structure elements showed a good fit. The Tt-SerRS structure was used as a reference to guide the initial model building. Density for the N-terminal domain was visible after refinement; model building was carried out in O (Jones *et al*, 1991). Several cycles of model building and refinement followed by automatic/manual water picking resulted in a final model including residues 1–502 for both molecules, except for two loops in one chain, residues 12–21 and 51–56, for which no interpretable electron density was found. In addition to these, two-loop residues 83–95 were disordered in the structure with serine or Ser-AMS. In the case of apo-enzyme and enzyme–ATP complex the 'serine ordering loop' residues are disordered. The model quality was analyzed by PROCHECK (Laskowski *et al*, 1993).

ATP-PP_i exchange assay

Amino-acid activation by aMb-SerRS was measured at 37°C in 100 mM Hepes (pH 7.0), 20 mM $MgCl_2$, 25 mM KCl, 4 mM ATP, 1 mM ^{32}P-PP_i (0.005–0.05 μCi/μl). Serine and threonine were varied between 12.5–750 μM and 12.5–500 mM, respectively, while the enzyme was 100 and 500 nM. The reaction was mixed with a quench solution prior to product separation by thin-layer chromatography on polyethyleneimine cellulose plates (Gruic-Sovulj *et al*, 2005; Uter *et al*, 2005). The dried chromatogram was quantified on a Molecular Dynamics Storm 840 phosphoimager and the kinetic data were obtained as described (Gruic-Sovulj *et al*, 2005).

ATP-hydrolysis assay

Stimulation of ATP hydrolysis in the presence of noncognate amino acid was measured at 37°C in 50 mM Hepes (pH 7.0), 25 mM KCl, 20 mM $MgCl_2$, 0.5 mM ^{32}P-ATP (0.05 μCi/μl) and 500 mM amino acid. aMb-SerRS and $tRNA^{Ser}$ *in vitro* transcripts were 1–2.5 μM and 2.5–7 μM, respectively. In the control reaction, serine was 1 mM. Reaction was quenched, subjected to the thin-layer analysis and data were analyzed as described (Gruic-Sovulj *et al*, 2005).

Alanine-scanning mutagenesis and enzyme kinetics

The site-directed mutagenesis was performed using the Quick-Change system (Stratagene). Mutated enzymes were overexpressed, purified and the serylation activity was tested as described (Korencic *et al*, 2004b).

Coordinates

The atomic coordinates and structure factors have been deposited in the Protein Data Bank. The accession code is 2cim for aMb-SerRS-apo, 2cja for aMb-SerRS:ATP, 2cjb for aMb-SerRS:serine and 2cj9 for aMb-SerRS:SSA.

Supplementary data

Supplementary data are available at *The EMBO Journal* Online.

Acknowledgements

Data collection was performed at the Swiss Light Source (SLS) of the Paul Scherrer Institut (PSI) in Villigen. We are grateful to C Schulze-Briese, T Tomizaki and A Wagner at the SLS whose outstanding efforts have made these experiments possible. This work was supported by the Scientific Co-operation between Eastern Europe and Switzerland (SCOPES) program of the Swiss National Science Foundation (SNSF), the NCCR Structural Biology program of the SNSF, a Young Investigator grant from the Human Frontier Science Program to NB and by the Ministry of Science, Education and Sports of the Republic of Croatia. SB was a recipient of UNESCO/L'OREAL fellowship.

References

Ahel D, Slade D, Mocibob M, Söll D, Weygand-Durasevic I (2005) Selective inhibition of divergent seryl-tRNA synthetases by serine analogues. *FEBS Lett* **579:** 4344–4348

Arnez JG, Dock-Bregeon AC, Moras D (1999) Glycyl-tRNA synthetase uses a negatively charged pit for specific recognition and activation of glycine. *J Mol Biol* **286:** 1449–1459

Baldwin AN, Berg P (1966) Transfer ribonucleic acid-induced hydrolysis of valyladenylate bound to isoleucyl ribonucleic acid synthetase. *J Biol Chem* **241:** 839–845

Baron B, Bock B (1995) The selenocysteine-inserting tRNA species: structure and function. In *tRNA: Structure, Biosynthesis and Function*, Söll D, RajBhandary U (eds), pp 529–544. Washington, DC: American Society for Microbiology

Beebe K, Merriman E, Ribas de Pouplana L, Schimmel P (2004) A domain for editing by an archaebacterial tRNA synthetase. *Proc Natl Acad Sci USA* **101:** 5958–5963

Belrhali H, Yaremchuk A, Tukalo M, Berthet-Colominas C, Rasmussen B, Bösecke P, Diat O, Cusack S (1995) The structural bases for seryl-adenylate and Ap_4A synthesis by seryl-tRNA synthetase. *Structure* **3:** 341–352

Belrhali H, Yaremchuk A, Tukalo M, Larsen K, Berthet-Colominas C, Leberman R, Beijer B, Sproat B, Als-Nielsen J, Grubel G, Legrand J-F, Lechmann M, Cusack S (1994) Crystal structures at 2.5 Angstrom resolution of seryl-tRNA synthetase complexed with two analogs of seryl adenylate. *Science* **263:** 1432–1436

Bilokapic S, Korencic D, Söll D, Weygand-Durasevic I (2004) The unusual methanogenic seryl-tRNA synthetase recognizes $tRNA^{Ser}$ species from all three kingdoms of life. *Eur J Biochem* **271:** 694–702

Biou V, Yaremchuk A, Tukalo M, Cusack S (1994) The 2.9 Å crystal structure of *T. Thermophilus* seryl-tRNA synthetase complexed with $tRNA^{Ser}$. *Science* **263:** 1404–1410

Borel F, Vincent C, Leberman R, Härtlein M (1994) Seryl-tRNA synthetase from *Escherichia coli*: implication of its N-terminal domain in aminoacylation activity and specificity. *Nucleic Acids Res* **22:** 2963–2969

Chimnaronk S, Jeppesen MG, Suzuki T, Niborg J, Watanabe K (2005) Dual-mode recognition of noncanonical $tRNA^{Ser}$ by seryl-tRNA synthetase in mammalian mitochondria. *EMBO J* **24:** 3369–3379

Collaborative Computational Project, N (1994) The CCP4 suite: programs for protein crystallography. *Acta Crystallogr D* **50:** 760–763

Cowtan K (1994) Joint CCP4 and ESF-EACBM. *Newslett Protein Crystallogr* **31:** 34–38

Cusack S (1993) Sequence, structure and evolutionary relationships between class 2 aminoacyl-tRNA synthetases: an update. *Biochimie* **75:** 1077–1081

Cusack S, Berthet-Colominas C, Härtlein M, Nassar N, Leberman R (1990) A second class of synthetase structure revealed by X-ray analysis of *Escherichia coli* seryl-tRNA synthetase at 2.5 Å. *Nature* **347:** 249–255

Cusack S, Härtlein M, Leberman R (1991) Sequence, structural and evolutionary relationships between class 2 aminoacyl-tRNA synthetases. *Nucleic Acids Res* **13:** 3489–3498

Cusack S, Yaremchuk A, Tukalo M (1996) The crystal structure of the ternary complex of *T. thermophilus* seryl-tRNA synthetase with $tRNA^{Ser}$ and a seryl-adenylate analogue reveals a conformational switch in the active site. *EMBO J* **15:** 2834–2842

Dock-Bregeon A-C, Rees B, Torres-Larios A, Bey G, Caillet J, Moras D (2004) Achieving error-free translation: the mechanism of proofreading of threonyl-tRNA synthetase at atomic resolution. *Mol Cell* **16:** 375–386

Dock-Bregeon A-C, Sankaranarayanan R, Romby P, Caillet J, Springer M, Rees B, Francklyn CS, Ehresmann C, Moras D (2000) Transfer-RNA-mediated editing in threonyl-tRNA synthetase: the class II solution to the double discrimination problem. *Cell* **103:** 877–884

Eriani G, Delarue M, Poch O, Gangloff J, Moras D (1990) Partition of tRNA synthetases into two classes based on mutually exclusive sets of sequence motifs. *Nature* **347:** 203–206

Fujinaga M, Berthet-Colominas C, Yaremchuk AD, Tukalo MA, Cusack S (1993) Refined crystal structure of the seryl-tRNA synthetase from *Thermus thermophilus* at 2.5 Å resolution. *J Mol Biol* **234:** 222–233

Gruic-Sovulj I, Luedemann HC, Hillenkamp F, Weygand-Durasevic I, Kucan Z, Peter-Katalinic J (1997) Detection of noncovalent tRNA:aminoacyl-tRNA synthetase complexes by matrix assisted laser desorption/ionization mass spectrometry. *J Biol Chem* **272:** 32084–32091

 ©2006 European Molecular Biology Organization

Gruic-Sovulj I, Uter N, Bullock T, Perona JJ (2005) tRNA-dependent aminoacyl-adenylate hydrolysis by a nonediting class I aminoacyl-tRNA synthetase. *J Biol Chem* **280:** 23978–23986

Hauenstein S, Zhang CM, Hou Y-M, Perona JJ (2004) Shape-selective RNA recognition by cysteinyl-tRNA synthetase. *Nat Struct Mol Biol* **11:** 1134–1141

Helm M, Brule H, Friede D, Giege R, Putz D, Florentz C (2000) Search for characteristic structural features of mammalian mitochondrial tRNAs. *RNA* **6:** 1356–1379

Ibba M, Söll D (2000) Aminoacyl-tRNA synthesis. *Ann Rev Biochem* **69:** 617–650

Jones TA, Zou JY, Cowan SW, Kjeldgaard M (1991) Improved methods for building protein models in electron density maps and the location of errors in these models. *Acta Crystallogr A* **47:** 110–119

Kim H-S, Vothknecht UC, Hedderich R, Celic I, Söll D (1998) Sequence divergence of seryl-tRNA synthetases in archaea. *J Bacteriol* **180:** 6446–6449

Korencic D, Ahel I, Schelert J, Sacher M, Ruan B, Stathopoulos C, Blum P, Ibba M, Söll D (2004a) A freestanding proofreading domain is required for protein synthesis quality control in archaea. *Proc Natl Acad Sci USA* **101:** 10260–10265

Korencic D, Ahel I, Söll D (2002) Aminoacyl-tRNA synthesis in methanogenic archaea. *Food Technol Biotechnol* **40:** 235–260

Korencic D, Polycarpo C, Weygand-Durasevic I, Söll D (2004b) Differential modes of transfer RNA^{Ser} recognition in *Methanosarcina barkeri*. *J Biol Chem* **279:** 48780–48786

Laskowski RA, MacArthur MW, Moss DS, Thornton JM (1993) Procheck—a program to check the stereochemical quality of protein structures. *J Appl Crysallogr* **26:** 283

Lenhard B, Orellana O, Ibba M, Weygand-Durasevic I (1999) tRNA recognition and evolution of determinants in seryl-tRNA synthesis. *Nucleic Acids Res* **27:** 721–729

Otwinowski Z, Minor W (1997) Processing of X-ray diffraction data collected in oscillation mode. *Methods Enzymol* **276:** 307–326

Ribas de Pouplana L, Schimmel P (2001) Two classes of tRNA synthetases suggested by sterically compatible dockings on tRNA acceptor stem. *Cell* **102:** 191–193

Sankaranarayanan R, Dock-Bregeon A-C, Rees B, Bovee M, Caillet J, Romby P, Francklyn CS, Moras D (2000) Zinc ion mediated amino acid discrimination by threonyl-tRNA synthetase. *Nat Struct Biol* **7:** 461–465

Sauerwald A, Zhu W, Major TA, Roy H, Palioura S, Jahn D, Whitman WB, Yates JRR, Ibba M, Söll D (2005) RNA-dependent cysteine biosynthesis in archaea. *Science* **307:** 1969–1972

Sheldrick G, Schneider TR (1997) SHELXL: high resolution refinement. *Methods Enzymol* **277:** 319–343

Shimada N, Suzuki T, Watanabe K (2001) Dual mode recognition of two isoacceptor tRNAs by mammalian mitochondrial seryl-tRNA synthetase. *J Biol Chem* **276:** 46770–46778

Tang SN, Huang JF (2005) Evolution of different oligomeric glycyl-tRNA synthetases. *FEBS Lett* **579:** 1441–1445

Terwilliger TC (2002) Automated main-chain model-building by template-matching and iterative fragment extension. *Acta Crystallogr D* **59:** 34–44

Thompson JD, Gibson TJ, Plewniak F, Jeanmougin F, Higgins DG (1997) The CLUSTALX Windows interface: flexible strategies for multiple sequence alignment aided by quality analysis tools. *Nucleic Acids Res* **25:** 4876–4882

Torres-Larios A, Sankaranarayanan R, Rees B, Dock-Bregeon A-C, Moras D (2003) Conformational movements and cooperativity upon amino acid, ATP and tRNA binding in threonyl-tRNA synthetase. *J Mol Biol* **331:** 201–211

Tsui W-C, Fersht AR (1981) Probing the principles of amino acid selection using the alanyl-tRNA synthetase from *Escherichia coli*. *Nucleic Acids Res* **9:** 4627–4637

Tumbula D, Vothknecht UC, Kim H-S, Ibba M, Min B, Li T, Pelaschier J, Stathopoulos C, Becker H, Söll D (1999) Archaeal aminoacyl-tRNA synthesis: diversity replaces dogma. *Genetics* **152:** 1269–1276

Uter NT, Gruic-Sovulj I, Perona JJ (2005) Amino acid-dependent transfer RNA affinity in a class I aminoacyl-tRNA synthetase. *J Biol Chem* **280:** 23966–23977

Vincent C, Borel F, Willson JC, Leberman R, Härtlein M (1995) Seryl-tRNA synthetase from *Escherichia coli*: functional evidence for cross-dimer binding during aminoacylation. *Nucleic Acids Res* **23:** 1113–1118

Weygand-Durasevic I, Cusack S (2005) Structure, function and evolution of seryl-tRNA synthetases. In *The Aminoacyl-tRNA Synthetases*, Ibba M, Francklyn C, Cusack S (eds), pp 177–192. Georgetown, TX: Landes Bioscience

Wintjens R, Rooman M (1996) Structural classification of HTH DNA-binding domains and protein–DNA interaction modes. *J Mol Biol* **262:** 294–313

Woese CR, Olsen GJ, Ibba M, Söll D (2000) Aminoacyl-tRNA synthetases, the genetic code, and the evolutionary process. *Microbiol Mol Biol Rev* **64:** 202–236

Wolf YI, Aravind L, Grishin NV, Koonin EV (1999) Evolution of aminoacyl-tRNA synthetases—analysis of unique domain architectures and phylogenetic trees reveals a complex history of horizontal gene transfer events. *Genome Res* **9:** 689–710

Yaremchuk A, Kriklivyi I, Tukalo M, Cusack S (2002) Class I tyrosyl-tRNA synthetase has a class II mode of cognate tRNA recognition. *EMBO J* **21:** 3829–3840

Yaremchuk A, Tukalo M, Groetli M, Cusack S (2001) A succession of substrate induced conformational changes ensures the amino acid specificity of *Thermus thermophilus* prolyl-tRNA synthetase: comparison with histidyl-tRNA synthetase. *J Mol Biol* **309:** 389–1002

©2006 European Molecular Biology Organization